

Article

Simulating Maize Productivity under Selected Climate Smart Agriculture Practices Using AquaCrop Model in a Sub-humid Environment

Alex Zizinga ^{1,*}, Jackson Gilbert Majaliwa Mwanjalolo ^{1,2}, Britta Tietjen ³, Bohe Bedadi ⁴, Ramon Amaro de Sales ⁵ and Dennis Beesigamukama ^{6,7}

- ¹ Africa Centre of Excellence for Climate Smart Agriculture and Biodiversity Conservation, Haramaya University, Dire Dawa P.O. Box 138, Ethiopia; m.majaliwa@ruforum.org
 - ² Regional Universities Forum for Capacity Building in Agriculture, Makerere University, Wandegaya, Kampala P.O. Box 16811, Uganda
 - ³ Institute of Biology, Theoretical Ecology, Freie Universität Berlin, Königin-Luise-Str. 2/4, Gartenhaus, D-14195 Berlin, Germany; britta.tietjen@fu-berlin.de
 - ⁴ College of Agriculture and Environmental Sciences, Haramaya University, Dire Dawa P.O. Box 138, Ethiopia; bobedadi2009@gmail.com
 - ⁵ Department of Plant Science, Federal University of Viçosa, Viçosa 36570-900, MG, Brazil; ramonamarodesales@gmail.com
 - ⁶ Department of Crop Production and Management, Busitema University, Soroti P.O. Box 203, Uganda; dbesiga@gmail.com
 - ⁷ International Centre of Insect Physiology and Ecology, Nairobi P.O. Box 30772-00100, Kenya
- * Correspondence: azizinga@gmail.com; Tel.: +256-774284497



Citation: Zizinga, A.; Mwanjalolo, J.G.M.; Tietjen, B.; Bedadi, B.; Amaro de Sales, R.; Beesigamukama, D. Simulating Maize Productivity under Selected Climate Smart Agriculture Practices Using AquaCrop Model in a Sub-humid Environment. *Sustainability* **2022**, *14*, 2036. <https://doi.org/10.3390/su14042036>

Academic Editor:
Nádia Luísa Castanheira

Received: 15 December 2021

Accepted: 2 February 2022

Published: 11 February 2022

Publisher's Note: MDPI stays neutral with regard to jurisdictional claims in published maps and institutional affiliations.



Copyright: © 2022 by the authors. Licensee MDPI, Basel, Switzerland. This article is an open access article distributed under the terms and conditions of the Creative Commons Attribution (CC BY) license (<https://creativecommons.org/licenses/by/4.0/>).

Abstract: Crop models are crucial in assessing the reliability and sustainability of soil water conservation practices. The AquaCrop model was tested and validated for maize productivity under the selected climate smart agriculture (CSA) practices in the rainfed production systems. The model was validated using final biomass (B) and grain yield (GY) data from field experiments involving seven CSA practices (halfmoon pits, 2 cm thick mulch, 4 cm thick mulch, 6 cm thick mulch, 20 cm deep permanent planting basins (PPB), and 30 cm deep) and the control (conventional practice) where no CSA was applied. Statistics for coefficient of determination (R^2), Percent bias (Pbias), and Nash–Sutcliffe (E) for B and GY indicate that the AquaCrop model was robust to predict crop yield and biomass as illustrated by the value of $R^2 > 0.80$, Pbias -1.52 – 1.25% and $E > 0.68$ for all the CSA practices studied. The relative changes between the actual and simulated water use efficiency (WUE) of grain yield was observed in most of the CSA practices. However, measured WUE was seemingly better in the 2 cm thick mulch, indicating a potential for water saving and yield improvement. Therefore, the AquaCrop model is recommended as a reliable tool for assessing the effectiveness of the selected CSA practices for sustainable and improved maize production; although, the limitations in severely low soil moisture conditions and water stressed environments should be further investigated considering variations in agroecological zones.

Keywords: climate smart agriculture practices; AquaCrop model; rainfed production systems and maize production

1. Introduction

The global population growth is expected to increase over the next 50 years and, hence, rise the demand for food [1]. This will necessitate an increase in agriculture production per unit land area, especially in the developing countries of sub-Saharan Africa (SSA) [2,3]. In SSA, food production, which is majorly dependent on natural rainfall, has been greatly affected by water stress related to rainfall fluctuation associated with climate change. Therefore, efforts to increase food production should address the challenges of water

shortages through improved soil water management strategies [4]. In Uganda, the situation is worsening because of the torrential (high intensity in a short time) nature of the rains often causing crop damage and soil erosion [3,5,6]. In some places in Uganda, the rainfall pattern is characterized by long dry spells (five months), which cause severe crop water stress during critical growth stages, leading to low crop yields or total crop failure.

Among the crops affected is maize, a major cereal crop that significantly contributes to food security and income generation in Uganda, whereby smallholder farmers account for 90% of the total production under natural rainfed conditions [7]. However, the increase in dry spells without supplemental water management practices in the cropping seasons affects maize productivity. The adoption of climate smart agriculture practices for soil water conservation could boost maize production in these areas.

Climate smart agriculture (CSA) practices are gaining momentum as an adaptation option to address the challenges of unreliable rainfall and water shortages in agriculture production while protecting the environment [8,9]. Climate smart agriculture practices refer to farm management practices that sustainably increase productivity, resilience, and reduce greenhouse gases to enhance the achievement of national food security and sustainable development goals [8]. The primary purpose of CSA is to transform and reorient existing agricultural systems to support food security under a changing climate [10]. These CSA practices have been used by farmers in humid, sub-humid, and dryland areas worldwide to increase soil moisture storage and boost agricultural productivity [9,11,12]. Numerous CSA practices including mulching, permanent planting basins, halfmoon pits, tied ridges, crop varieties, and irrigation have been used on cultivated land in different parts of SSA [10,12].

Despite the fact that CSA practices have been promoted, their adoption has remained very low due to lack of evidence on their efficiency over time among others [10,13]. In order to recommend some of these practices for future use aiming at sustaining crop production, crop simulation modeling is one of the alternatives and methods for testing the future efficiency of the CSA practices. Among many crop models available, the Food and Agriculture Organisation (FAO) AquaCrop simulation model provides a user-friendly interface and practitioner-oriented output to maintain optimal balance between accuracy, robustness, and simplicity [14]. The model has successfully simulated the growth, biomass, and yield of various crops such as maize [14–16], wheat [17], and soybean [18] under different climatic conditions.

The FAO AquaCrop simulation model also provides a sound theoretical framework to investigate, assess crop biomass, and yield response to various environmental conditions [15,19–22]. In Uganda, the FAO AquaCrop simulation model has specifically been employed to assess the impact of climate change and adaptation options on maize production [23]. However, there are conflicting reports on the performance of this model under different climatological zones [24,25]. This study, therefore, aimed to test and validate the AquaCrop model for maize under selected CSA practices in the tropical sub-humid environment of the mid-west Albert region of Uganda.

2. Materials and Methods

2.1. Field Experiments

A completely randomized block design field experiment was conducted at Bulindi Zonal Agriculture Research Development Institute, Western Uganda (1°00′–2°00′ N and 30°30′–31°45′ E, 1276 m asl) [26]. The climate of Bulindi is tropical, wet and dry with highly spatial and temporal rainfall distribution [27]. The study was conducted for three growing seasons and it was completely rainfed, whereby the first season begun in March 2019 and ended in August 2019 and was characterised by relatively long rains (Figure 1a). The second season ran from October 2019 to February 2020 (Figure 1b), while the third season started in March 2020 and ended in August 2020 (Figure 1c).

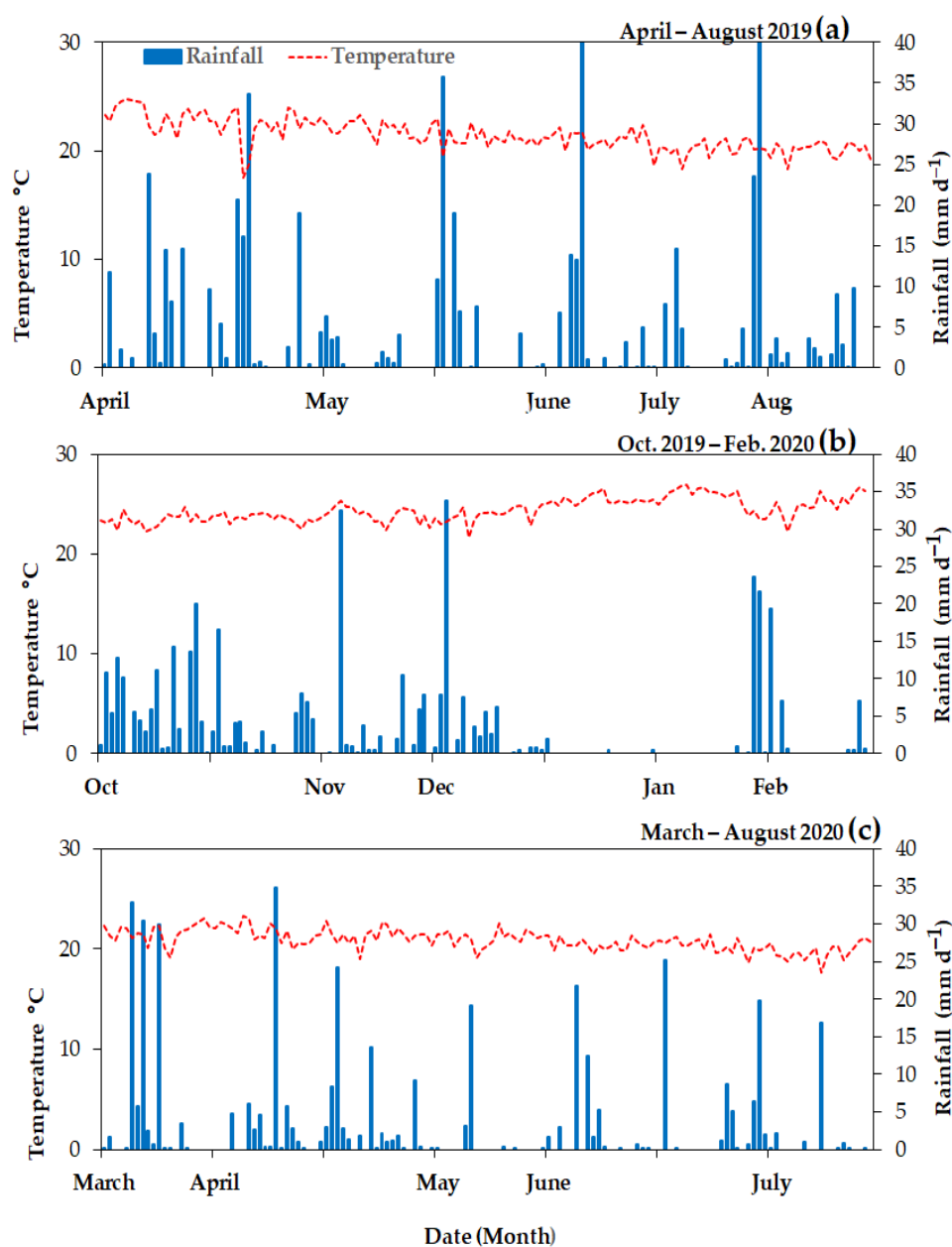


Figure 1. Rainfall recorded during the first (April–August 2019) (a), second (October 2019–February 2020) (b), and third (March–August 2020) (c) maize cropping seasons. Source: Field climate data collected in 2019–2020.

During the study period, data on daily rainfall, air temperature, humidity, wind speed (at 2 m height), and solar radiation were collected from a site installed weather station at Bulindi Zonal Agriculture Research Institute. The mean maximum temperature was 21.5 °C in season 1 (Figure 1a), 24.4 °C for season 2 (Figure 1b), and 20.9 for season 3 (Figure 1c). The temperature over seasons varied greatly between the months of June (20.1 °C), October (23.4 °C), and April to May (22.8 °C). The highest rainfall (529 mm) was recorded in the first season while the third season received the lowest rainfall (406 mm). Although the second season received higher rainfall (418 mm) than the third season, most of the rainfall was concentrated in two months (October and November in 2019) (Figure 1b).

2.2. CSA Treatments and Experimental Set Up

A completely randomized block design with four replications was used to establish the experiment (Figure 2). The experiment consisted of seven treatments, which included

grass mulch with thicknesses of 2 cm (M2 cm), 4 cm (M4 cm), and 6 cm (M6 cm), halfmoon (HM), permanent planting basins (PPB) of 20 cm (PPB20 cm) and 30 cm (PPB30 cm) depths, and the control.

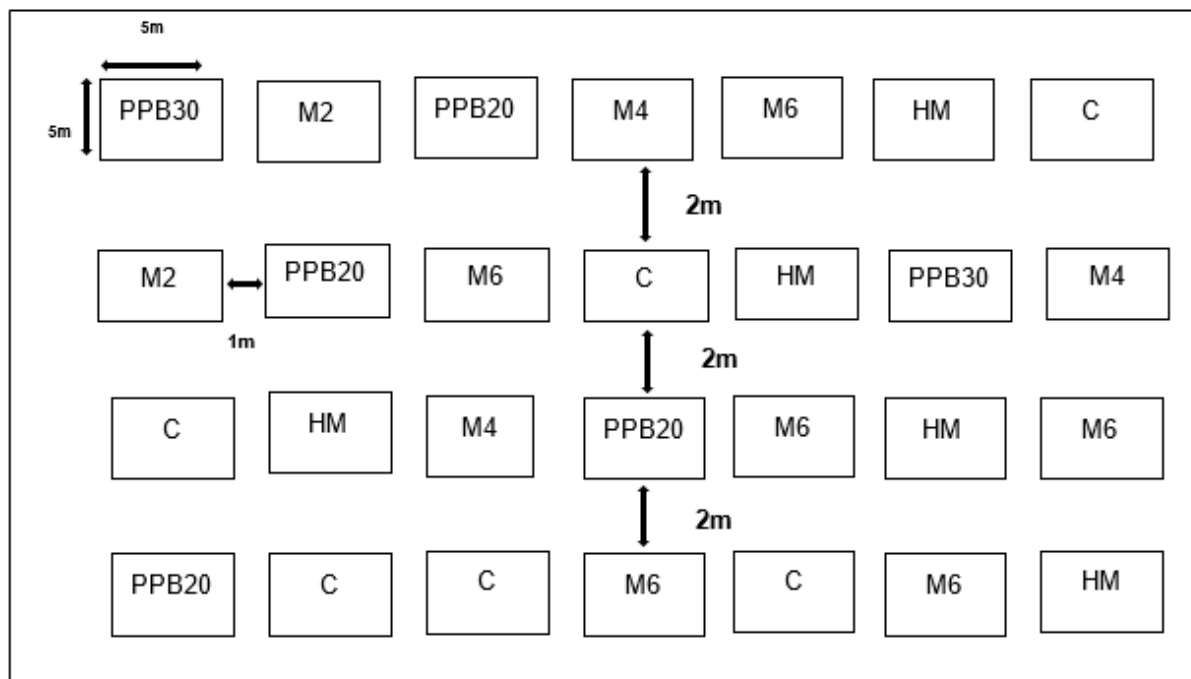


Figure 2. Experimental layout in field experiments with four treatments C = Control, HM = Half-moon, PPB 20cm = Permanent Planting basin circular pits of 15 cm diameter and depth of 20 cm; PPB 30cm = Permanent Planting basin circular pits of 15 cm diameter and 30 cm depth; M 2 cm, M 4 cm and M 6 cm = soil surface covered with 2 cm, 4 cm, and 6 cm thick layer of dry grass materials, respectively.

For mulching treatments, the soil in each plot was covered with dry grass materials to obtain thicknesses of 2 cm, 4 cm, and 6 cm above the soil surface. This was done immediately after sowing, such that the mulching materials were put between the rows. For the halfmoon treatment, six moon shaped pits measuring 30 cm deep, 50 cm wide, and 100 cm circumference were dug using a hand hoe at a spacing of 30 cm [10,28]. The permanent planting basin treatments were established by digging circular pits of 15 cm diameter and depths of 20 cm (PPB20 cm) and 30 cm (PPB 30 cm). The PPB treatments were established one day before sowing.

The control treatment comprised of a bare surface field without any water management technique, which is the conventional cultivation practice used in the study area. In all treatments, maize (Longe 9H variety) was sown 5 cm deep at spacing of 75 cm between rows \times 30 cm between hills on 1 April 2019, 5 October 2019, and 17 March 2020 for seasons one, two, and three, respectively.

Plots of 5 \times 5 m with borders of 1 m between plots and 2 m between blocks were used. To cater for the maize nutrient requirements, diammonium phosphate (60 kg ha⁻¹) and muriate of potash (60 kg ha⁻¹) were basally applied at blanket rates during sowing. At eight weeks after sowing, top dressing was conducted by applying urea fertilizer at a blanket rate of 90 kg ha⁻¹ [7,29]. The pests and diseases were controlled wherever they appeared while weeds were controlled by hand pulling. The study was repeated only for the long rain season while the short rain season experiment was not repeated.

2.3. Maize Growth and Yield

Data on aboveground biomass were collected at vegetative, tasseling, silking, and maturity stages in the three growing seasons and the cumulative soil moisture in each CSA

practice, respectively (Table 1). At vegetative, tasseling, and silking stages, biomass was determined using four maize plants selected from the outer plot rows. The maize shoot was cut off at the ground level and its weight determined using a weighing scale. At maturity, the above ground biomass and grain yield were measured in a 4 m² subplot. The maize shoots from the harvested area were weighed to obtain fresh weight immediately after harvesting. From each plot, sub samples of the grain and stover were collected and oven dried at 60 °C at Makerere University soil science laboratory until constant weight was obtained. The dry weights of maize biomass and grain were used to calculate the yields of maize biomass and grain yield on hectare basis (t ha⁻¹).

Table 1. Phenological growth stages and soil moisture in CSA treatments.

Agronomic Details	Season 1	Season 2	Season 3
Planting density	44,444	44,444	44,444
Sowing date	31 March 2019	5 October	17 March
Days to emergence	6	7	6
Days to vegetative stage	44	44	44
Days to tasseling	59	59	59
Days to silking	73	73	73
Days to maturity	140	140	140
Cumulative soil moisture (%)			
Control	20.6	35.9	36.3
Halfmoon	23.6	38.6	36.2
PPB20 cm	32.9	36.4	36.0
PPB30 cm	40.3	32.8	36.0
M2 cm	22.0	31.4	35.8
M4 cm	37.6	36.4	35.8
M6 cm	34.3	36.7	36.1

Key: Control = conventional practice without any water management technique; Halfmoon = moon shaped pits measuring 30 cm deep, 50 cm wide, and 100 cm circumference; PPB20 cm = circular pits of 15 cm diameter and depth of 20 cm; PPB30 cm = circular pits of 15 cm diameter and 30 cm depth; M2 cm = soil surface covered with 2 cm thick layer of dry grass materials; M4 cm = soil surface covered with 4 cm thick layer of dry grass materials; M6 cm = soil surface covered with 6 cm thick layer of dry grass materials.

2.4. AquaCrop Model

The model evolved through the approach of modelling crop yield and water [30]. The model links soil, crop, and water relations, for example rain, temperature, evapotranspiration, and carbon dioxide to existing environmental conditions together with plant growth characteristics (crop cover, phenology, root depth, biomass, and agronomic practices like fertilizer use and irrigation [16,31]). The AquaCrop model calculates daily water balance and separates evapotranspiration and transpiration. The non-productive water use is not considered in the simulation since actual evapotranspiration is computed. The model also allows the crop to respond to water stress through the stress coefficients embedded within the AquaCrop model engine, namely, leaf expansion, stomatal closure, canopy senescence, and harvest index. In addition, the model uses canopy cover from daily transpiration into leaf area development, hence, the canopy cover development, senescence, and harvest index are simulated [22,32,33]. The values within the model can be adjusted for different environmental conditions and related growth stress.

The changes in the soil water of the root zone enables the simulation of crop growth, its development and yield through the water balance approach, which considers incoming and outgoing water fluxes. The water stress coefficients are embedded in the AquaCrop as a function to account for water deficit in the rooting zone and this also relates to canopy expansion, senescence, and pollination [4].

2.4.1. Model Parameters and Inputs

Climate Data

The soil-water plant relation of the AquaCrop model relies on climate such as air temperature, rainfall, reference evapotranspiration (ET_0), and carbon dioxide. The ET_0 was computed by employing the FAO Penman–Monteith equation [34]. The minimum and maximum air temperature, wind speed, relative humidity, sunshine hours, and solar radiation were collected from the weather station at Bulindi agriculture research station.

Crop Characteristics

The crop evapotranspiration (ET_c) was calculated by multiplying the ET_0 with crop coefficient at each crop growth stage for the three growing seasons (Equation (1)) [34,35]. Since there were no site-specific K_c values for maize in the study area, we adopted the crop coefficient values of Food and Agriculture Organisation [34] for the four maize growth stages (initial, development, middle, and late stages).

$$ET_c = ET_0 \times \kappa_c \quad (1)$$

where,

ET_c represents the crop evapotranspiration (mm day^{-1}),

ET_0 represents the reference crop evapotranspiration (mm day^{-1}),

κ_c represents the crop coefficient (dimensionless).

The total length of maize growth was 140 days. The dates of maize growth stages were determined from phenology of the crop and its percentage ground cover. The growing period was divided into initial, development, middle, and late stages [34–36]. The initial stage was when plants occupied 10% ground cover while the crop development stage was when plants occupied 10% to 70% ground cover. The middle stage included flowering and grain filling with yield formation and the late stage consist of the ripening and harvest phase when there is effective full cover [34, 35]. K_c values ranged between 0.3 to 1.2.

The ground water table was below the effective rooting depth, thus, the effects of water through capillary rise are not simulated. Moreover, the information relating to studied climate smart agriculture practices for all the three growing seasons was included in the AquaCrop model. The crop input in the model consisted of conservative parameters and non-conservative parameters such as planting density, germination, flowering, and maturity time, yield, root depth, and the harvest index.

In this study, crop parameters included the crop canopy cover, biomass for water productivity, coefficients of crop transpiration and response of water stress and the stomatal closure all embedded in the AquaCrop model. The percentage canopy cover is estimated in the model using methods proposed by Farahani et al. [19] and Steduto et al. [21,37]. Since the first season was conducted in the anticipated long-term rains (March to August 2019) where waterlogging is anticipated to occur, the consideration of aeration stress was inevitable. Exceeding the anaerobiosis point in the root zone results in decrease in transpiration [4,21].

Soil Characteristics

The soil data included soil water characteristics like volumetric water contents at the permanent wilting point, saturation, field capacity, and hydraulic conductivity of the soil at depths 10 cm, 20 cm, 30 cm, and 40 cm. Measurements of water contents of the soil were conducted using the Frequency-Domain-Reflectometry (FDR) profile probe-type PR2/4 [38], while the saturated soil water conductivity (K_{sat}) was determined using the water permeameter [39]. The Rosetta pedotransfer function was also used to estimate the hydraulic parameters using soil texture data [40]. The K_{sat} , bulk density, field capacity, and permanent wilting point were used as initial estimates. All the mentioned soil parameters were determined following standard procedures.

2.4.2. Model Calibration and Validation

Assessment of the performance and robustness of the AquaCrop model under varying crop growing conditions was achieved by comparing the biomass accumulation, grain yield, ET_c , and WUE of maize against field measurements and estimations in the CSA treatments. All the simulations were limited to the conditions of no nutrient and salinity stress in the AquaCrop (v. 6.1).

As a first step, the model was calibrated using season 3 outputs from the control experiment and validated using seasons 1 and 2. The procedure was an iterative process of adjusting sensitive parameters, mainly non-conservative parameters in the AquaCrop and assessing both the absolute and relative difference. For each change in input, simulations were run using the calibrated crop file and the corresponding CSA treatment. The recent study [15,41] reports the most sensitive parameters in the AquaCrop obtained through sensitivity analysis testing similar to those in Table 2. The main parameters used to calibrate the AquaCrop model for simulating maize growth and productivity for the study location are presented in Table 2. The harvest index of 48%, which was used in the model, is comparable to those of previous studies [4].

Since the study area was flat, runoff was negligible and the options were selected in the AquaCrop model under field management options.

Table 2. AquaCrop calibrated values for main parameters used in maize simulation.

Crop Variables	Value
Base temperature (°C)	9
Upper temperature (°C)	34
Maximum rooting depth (m)	0.45
Effect of canopy cover in late season (dimensionless)	60
Soil surface covered by an individual seedling at 90% emergence (cm ²)	5
Plant population per hectare	44,444
Canopy growth coefficient per day (dimensionless)	0.10988
Maximum canopy cover (%)	0.84
Canopy decline coefficient per day (dimensionless)	0.1003
Germination days	6
Planting days to maximum root depth	61
Days to senescence stage	114
Maturity period (days)	140
Days to flowering	59
Length of flowering stage	8
Period from building up of Harvest Index (days)	81
Reference Harvest Index (HI ₀) (%)	48
Water Productivity normalized for ET_0 and CO ₂ (gram/m ²)	30.5

2.4.3. Model Evaluation

The statistical indices were used to evaluate the AquaCrop model and they included (1) the coefficient of determination (R^2), (Equation (2)); (2) the Nash–Sutcliffe efficiency (E) (Equation (3)) [42]; (3) the Willmott Index of Agreement; (4) (Equation (4)) [43]; and (5) the root mean square error (RMSE) (Equation (5)) [44]. Proportions of model variance were determined using the R^2 , which ranged between 0 and 1.0, with high values indicating low variance of error [14]. The E was used to indicate efficiency of the model and determine the relative scale of residual variance between the observed and simulated maize grain yield or biomass [45]. According to Schaap et al. [40], E of 1.0 indicates the best fit for the observed and simulated data [46].

The d estimates the degree of relative error between observed and simulated values from the model predictions. The values of d range from 0 to 1.0, whereby 0 indicates disagreement while 1 shows a perfect model agreement. The percentage bias (Pbias) (Equation (6)) was also used to assess the deviation between observed and simulated values in the CSA treatments. The optimal value of Pbias is 0%, with positive and negative values indicating model underestimation and overestimation bias, respectively [46].

In addition to the above quantitative statistics for model evaluation, the *RMSE* (Equation (5)) was considered as a statistical measure of the error differences between measured and simulated values. It shows the overall deviation of values and indicated the model uncertainty [41]. The unit of measurement is similar to the observations and simulated variables, the values near 0 represent a very good model performance and vice versa.

$$R^2 = \frac{[\sum_{i=1}^n (O_i - \bar{O})(S_i - \bar{S})]^2}{\sum_{i=1}^n (O_i - \bar{O})^2 \times \sum_{i=1}^n (S_i - \bar{S})^2} \quad (2)$$

$$E = 1 - \frac{\sum_{i=1}^n (O_i - S_i)^2}{\sum_{i=1}^n (O_i - \bar{O})^2} \quad (3)$$

$$d = 1 - \frac{\sum_{i=1}^n (O_i - S_i)^1}{\sum_{i=1}^n (O_i - \bar{O})^1} \quad (4)$$

$$RMSE = 1 - \frac{\sum_{i=1}^n (O_i - S_i)^2}{n} \quad (5)$$

$$Pbias = 1 - \frac{\sum_{i=1}^n (O_i - S_i)}{\sum_{i=1}^n (O_i)} \times 100 \quad (6)$$

where, O_i is the measured and S_i is the simulated data, \bar{O} is the average measured, and \bar{S}_i is the simulated data, and n is the total number of measurements or observations. The closer the index value is to one, the better the agreement between the two variables that are being compared and vice versa.

3. Results

3.1. Soils of the Study Area

The soil type at the study site were Ferralsols with a bulk density of 1.34 g cm^{-3} . The predominant soil texture is clay according to the United States Department of Agriculture classification [47]. The average field capacity, permanent wilting point, and saturation were 25.2%, 19.9%, and 37.9%, respectively. Before the onset of experiments, soil at the experimental site was characterized for physical soil properties following recommended laboratory methods (Table 3).

Table 3. Soil water characteristics of the study site.

Soil Hydraulic Properties	Soil Depth (cm)			
	0–10	10–20	20–30	30–40
Saturated hydraulic conductivity (mm day^{-1})	832.2	837.0	848.8	856.2
Field capacity (% Vol)	24.0	20.5	26.7	29.7
Permanent wilting point (% Vol)	19.6	20.5	20.2	19.1
Saturation (% Vol)	35.8	36.3	38.6	41.0

3.2. The AquaCrop Model Performance Indicators for Total Maize Biomass Model Calibration and Validation

The statistical indices used to calibrate the model are presented in Table 4. The root mean square error (*RMSE*) and percentage bias (*Pbias*) were in the range of 1.21–2.74 and -0.54% – 1.36% , respectively (Table 4), in all the CSA practices. The PPB 20 cm treatment had the least *Pbias* while the control had the highest *Pbias*. The control treatment had lower values of Nash–Sutcliffe efficiency (*E*) and Willmott index of agreement (*d*) compared to other CSA practices (Table 4). The coefficient of determination (R^2) for the calibrated dataset between simulated and measured R^2 values range was 0.66–0.96, whereby the M 6 cm, M 4 cm, and M 2 cm had the highest and control treatment with the lowest values, respectively (Table 4).

Table 4. Statistical indices of the AquaCrop results for the calibrated total maize biomass.

Variables	C	HM	PPB 20 cm	PPB 30 cm	M 2 cm	M 4 cm	M 6 cm
RMSE	2.50	1.94	1.50	2.35	1.63	1.43	1.21
Pbias	1.46	0.98	0.70	1.36	1.31	−0.54	−0.55
<i>d</i>	0.86	0.94	0.97	0.92	0.96	0.97	0.98
<i>E</i>	0.46	0.80	0.89	0.69	0.82	0.91	0.93
R^2	0.66	0.85	0.92	0.80	0.95	0.95	0.96

Key: *RMSE* = Root mean square error, *Pbias* % = percentage bias, *d* = Willmott index of agreement, R^2 = Coefficient of determination, *E* = Nash–Sutcliffe efficiency, C = conventional practice without any water management technique; HM = moon shaped pits measuring 30 cm deep, 50 cm wide, and 100 cm circumference; PPB 20 cm = circular pits of 15 cm diameter and depth of 20 cm; PPB 30 cm = circular pits of 15 cm diameter and 30 cm depth; M 2cm = soil surface covered with 2 cm thick layer of dry grass materials; M 4 cm = soil surface covered with 4 cm thick layer of dry grass materials; M 6 cm = soil surface covered with 6 cm thick layer of dry grass materials.

The reliability under control treatment lessened, indicating water shortages. The relatively lower coefficient of determination (R^2) and low Nash–Sutcliffe efficiency (*E*) values for the control treatment compared to other CSA practices. The validated dataset, for simulated and measured data had an overall $R^2 = 0.83$ for the control treatment (Tables 4 and 5).

Table 5. Statistical indices of the AquaCrop results for the validated total maize biomass.

	C	HM	PPB 20 cm	PPB 30 cm	M 2 cm	M 4 cm	M 6 cm
RMSE	1.88	1.64	2.74	0.94	2.24	1.27	1.38
Pbias	1.25	0.62	−1.52	0.65	0.96	0.89	0.76
<i>d</i>	0.92	0.95	0.92	0.98	0.90	0.97	0.97
<i>E</i>	0.72	0.83	0.72	0.93	0.68	0.88	0.89
R^2	0.83	0.89	0.88	0.97	0.80	0.94	0.96

Key: *RMSE* = Root mean square error, *Pbias* % = percentage bias, *d* = Willmott index of agreement, R^2 = Coefficient of determination, *E* = Nash–Sutcliffe efficiency, C = conventional practice without any water management technique; HM = moon shaped pits measuring 30 cm deep, 50 cm wide, and 100 cm circumference; PPB 20 cm = circular pits of 15 cm diameter and depth of 20 cm; PPB 30 cm = circular pits of 15 cm diameter and 30 cm depth; M 2 cm = soil surface covered with 2 cm thick layer of dry grass materials; M 4 cm = soil surface covered with 4 cm thick layer of dry grass materials; M 6 cm = soil surface covered with 6 cm thick layer of dry grass materials.

Other R^2 values obtained in CSA practices and their relationships between the measured total maize biomass and individual treatments were above 0.80. However, the control treatment had lower *E* (0.46). There was generally a good model fit for all treatments, except the control (Table 4). During model validation, the control treatment had relatively lower R^2 compared to all the CSA practices (Table 4). It was also noted that values of percentage bias achieved using control treatment were also the highest. The M 2 cm, control, and PPB 20 cm treatments had the lowest values of *E* while M 6 cm and PPB 30 cm had the highest values for the coefficients of determination of 0.97 and 0.96 (Table 4).

The accuracy of the model was also further assessed using correlation analysis (Figure 3a,b). The overall correlation between the measured and simulated biomass at maturity was medium (0.57) (Figure 3a), while there was a strong positive correlation (0.77) between the measured and simulated values of grain yield (Figure 3b).

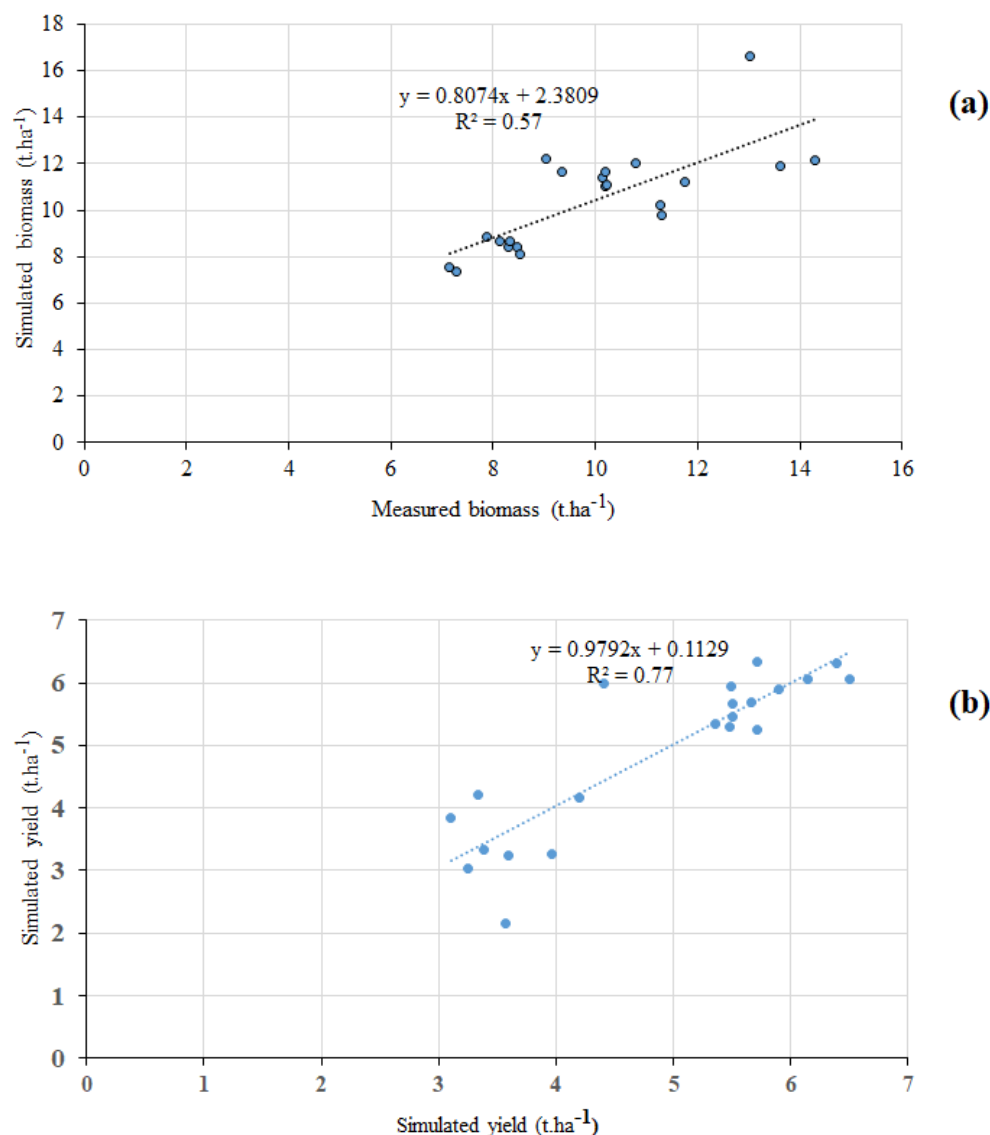


Figure 3. Correlation between measured and simulated values of maize biomass (a) and measured and simulated values of maize grain yield (b) during the AquaCrop model evaluation.

3.3. Biomass and Grain Yield

3.3.1. Calibrated Data Set

The measured and simulated values of biomass and grain yield are presented in Table 6. The measured values of aboveground maize biomass were 8.1–11.3 t ha⁻¹, while the simulated values ranged between 8.7 and 12 t ha⁻¹ (Table 6). All CSA practices produced higher total biomass than the control. The highest value of measured total biomass was harvested from plots treated with M 2 cm, while PPB 20 cm had the highest simulated total biomass. The deviation between measured and simulated values of total biomass ranged from −13.5 to 14.4%. The CSA practices M 2 cm and M 4 cm had the lowest and highest deviation in total biomass, respectively (Table 6).

The measured grain yield ranged between 4.2 and 5.7 t ha⁻¹, whereby the control produced the lowest grain yield while treatments M 2 cm and M 4 cm highest values. The values of measured grain achieved using M 2 cm and M 4 cm, and halfmoon, PPB 20 cm and M 6 cm were similar. The simulated values of grain yield ranged between 4.2 and 6.3 t ha⁻¹. All CSA practices had higher simulated values of grain yield than the control. The M 4 cm CSA practice had the highest value of simulated maize grain yield.

The relative change between measured and simulated values of grain yield ranged between -8.4 and 10.6% , treatments M 2 cm and M 4 cm had the lowest and highest values of deviation, respectively (Table 5). All treatments had negative values of relative change, except PPB 20 cm, M 4 cm, and M 6 cm.

Table 6. Simulated maize biomass and grain yield at harvest for CSA treatments for the calibrated dataset.

CSA Practices	Total Biomass (t ha^{-1})		Relative Change (%)	Grain Yield (t ha^{-1})		Relative Change (%)
	Measured	Simulated		Measured	Simulated	
C	8.1 ± 0.8	8.65	6.53	4.2 ± 0.7	4.2	-1.05
HM	10.1 ± 0.2	11.43	12.82	5.5 ± 0.7	5.5	-0.75
PPB 20 cm	10.8 ± 0.7	12.00	11.15	5.5 ± 0.6	5.7	2.76
PPB 30 cm	10.2 ± 2.1	11.01	7.86	5.4 ± 0.4	5.3	-0.21
M 2 cm	11.3 ± 1.6	9.77	-13.51	5.7 ± 0.7	5.2	-8.41
M 4 cm	10.2 ± 0.1	11.67	14.43	5.7 ± 0.7	6.3	10.60
M 6 cm	10.2 ± 1.0	11.09	8.58	5.5 ± 0.7	5.9	8.12

Key: C = Control, conventional practice without any water management technique; HM = Halfmoon shaped pits measuring 30 cm deep, 50 cm wide and 100 cm circumference; PPB 20 cm = circular pits of 15 cm diameter and depth of 20 cm; PPB 30 cm = circular pits of 15 cm diameter and 30 cm depth; M 2 cm = soil surface covered with 2 cm thick layer of dry grass materials; M 4 cm = soil surface covered with 4 cm thick layer of dry grass materials; M 6 cm = soil surface covered with 6 cm thick layer of dry grass materials.

3.3.2. Validated Data Set

Maize simulated biomass and grain yields are shown in Table 7. It ranged between 9 – 11 t ha^{-1} . The M 6 cm treatment produced higher biomass than all other CSA practices while M 2 cm and PPB 30 cm treatments were relatively lower. Moreover, treatment PPB 20 produced the highest values of simulated biomass compared to all the CSA practices (Table 7).

Table 7. Simulated compared values of biomass and grain yield at harvest in CSA practices for the validated dataset.

CSA Practices	Total Biomass (t ha^{-1})		Relative Change (%)	Grain Yield (t ha^{-1})		Relative Change (%)
	Measured	Simulated		Measured	Simulated	
C	10.0 ± 1.4	9.8	-1.76	4.6 ± 0.7	4.5	-0.6
HM	8.9 ± 2.3	10.0	12.1	4.0 ± 0.4	4.1	-2.0
PPB 20 cm	10.2 ± 1.1	12.0	14.4	5.0 ± 0.8	4.6	-9.0
PPB 30 cm	9.2 ± 1.0	8.9	-1.7	4.4 ± 0.4	4.2	-5.1
M 2 cm	8.7 ± 0.7	10.4	19.6	4.9 ± 0.5	5.3	12.3
M 4 cm	11.1 ± 0.5	10.0	-8.8	4.6 ± 0.7	5.0	11.0
M 6 cm	11.1 ± 0.6	10.5	-1.5	5.1 ± 0.7	4.6	-8.5

Key: C = Control, conventional practice without any water management technique; HM = Halfmoon shaped pits measuring 30 cm deep, 50 cm wide, and 100 cm circumference; PPB 20 cm = circular pits of 15 cm diameter and depth of 20 cm; PPB 30 cm = circular pits of 15 cm diameter and 30 cm depth; M 2 cm = soil surface covered with 2 cm thick layer of dry grass materials; M 4 cm = soil surface covered with 4 cm thick layer of dry grass materials; M 6 cm = soil surface covered with 6 cm thick layer of dry grass materials.

The measured grain yield ranged between 4 and 5.1 t ha^{-1} with M6 cm and PPB 20 cm having the highest grain yield (Table 7). The lowest values of measured grain yield were recorded from plots treated with halfmoon and control treatments. Simulated grain yields M 2 cm and M 4 cm was the highest during model validation compared to all the CSA practices. Under M 2 cm, grain yield increased by 18% and 11% for the M 4 cm from the control treatment. Moreover, the M 6 cm and PPB 20 cm increased grain yield by only 2% while the halfmoon and PPB 30 cm did not increase the grain yield from the control treatment (Table 7). In comparison, measured yield increased from the control by 24% for

M 4 cm and M 6 cm treatments (Table 7). The PPB 20 cm treatment increased grain yield also by only 4%.

3.4. Crop Evapotranspiration and Water Use Efficiency

Overall, the average crop evapotranspiration (ET_c) was 554 mm and 379 mm from validation and calibration datasets of the AquaCrop model (Table 8). During the validation exercise, a difference of 119 mm of ET_c was observed between the validated and calibrated ET_c . The average measured water use efficiency (WUE) observed was 12 kg mm⁻¹ ha⁻¹ and 10 kg mm⁻¹ ha⁻¹ for the validated and calibrated data, respectively. The AquaCrop model was robust in estimating WUE in all the CSA treatments as observed (Table 8). In the validated database, WUE also increased from the control treatment by 13%, 9%, and 1% under PPB 20 cm, M 4 cm and HM treatments, respectively, while other CSA practices did not increase WUE in the field observations. For the simulated WUE, the increase was 50%, 42%, 39%, and 19% for M 4 cm, M 6 cm, PPB 20 cm, and M 2 cm, respectively. Only PPB30 cm and the HM treatments did not show increase of WUE from the AquaCrop model simulated data (Table 8).

Table 8. Crop evapotranspiration and water use efficiency.

CSA Practice	ET_c (mm)			WUE (kg mm ⁻¹ ha ⁻¹)		
	Measured	Simulated	Relative Change (%)	Measured	Simulated	Relative Change (%)
Calibrated						
C	379	380	0.4	8.4	4.7	-44
HM	379	378	-0.2	10.9	7.4	-32
PPB 20 cm	379	379	0	14.5	10.8	-25
PPB 30 cm	379	379	0	10.6	7.7	-28
M 2 cm	379	379	0	10.9	10.3	-6
M 4 cm	379	379	0	15.1	15.8	5
M 6 cm	379	379	0	14.5	15.3	6
Validation						
C	554	507	-8	8	5	-33
HM	554	507	-8	8	5	-28
PPB 20 cm	554	446	-15	8	7	-19
PPB 30 cm	554	508	-8	6	4	-22
M 2 cm	554	507	-8	8	6	-21
M 4 cm	554	508	-5	8	8	-4
M 6 cm	554	507	-6	6	7	24

Key: C = Control, conventional practice without any water management technique; HM = Halfmoon shaped pits measuring 30 cm deep, 50 cm wide, and 100 cm circumference; PPB 20 cm = circular pits of 15 cm diameter and depth of 20 cm; PPB 30 cm = circular pits of 15 cm diameter and 30 cm depth; M 2 cm = soil surface covered with 2 cm thick layer of dry grass materials; M 4 cm = soil surface covered with 4 cm thick layer of dry grass materials; M 6 cm = soil surface covered with 6 cm thick layer of dry grass materials.

4. Discussion

Findings from the model simulation show that maize production using the control treatment was affected by relatively low soil moisture content. However, maize productivity simulated better using CSA practices, indicating better model performance under moderately low soil moisture content, water stressed, and non-stressed environment conditions. This is confirmed by the statistical indicators of root mean square error ($RMSE$), Nash–Sutcliffe efficiency (E), and Willmott index of agreement (d) observed during the calibration process (Table 4). It is also further corroborated by the simulation results in the present study and past studies, which show that the performance of the AquaCrop depends on the water shortages and stress levels experienced by the plants during the crop growth cycle [48].

The statistical analysis of the comparison between the measured and simulated final biomass showed high R^2 (0.77), indicating that the model predicted final biomass with a good degree of accuracy. The results of model validation indicate generally good fit between the measured and predicted datasets across CSA practices, except for the control treatment (Table 5). This is relatively due to low soil moisture content experienced in the

control treatment resulting in lower model efficiency. The values of d and E obtained during the study (Table 5) also indicate that the model was robust in simulating biomass and grain yield in different CSA practices.

The decline in model performance under reduced soil moisture content could also be attributed to reduced leaf water potential to -1.2Mpa , below which the AquaCrop model is unable to predict maize grain yield [15,24]. Due to low soil water content in the control treatment, the yield is affected, and this suggests that the model was not able to simulate the temporary recovery from water shortage due to insufficient soil water conservation in the control treatment and this corroborates with previous studies [19,22,49], where low soil moisture availability resulted into low yield and water use efficiency in non-irrigated treatments. In addition, Figure 1 indicates lower seasonal rainfall (406–529 mm) during seasonal experiments than the amount (500–800 mm/season) required for optimum maize production [34]. The relative changes in the observed and simulated biomass under halfmoon, PPB 20 cm, and M 4 cm could be the differences in soil moisture storage. The relatively higher changes between observed and simulated biomass under M 4 cm can be attributed to reduced mulch thickness arising from termite degradation of grass materials, which exposed the soil to solar radiation and increased evaporation (Table 7). The shallow depth of treatment PPB 20 cm could have reduced soil moisture storage and caused water stress due to higher evaporative loss and this is also related to previous studies of He et al., [50,51].

In addition, the relative increases of the AquaCrop simulation model for maize biomass under PPB 20 cm and M 4 cm CSA practices may be attributed to overestimation of stomatal conductance by the model [52]. This process allows plants to increase carbon dioxide uptake, which subsequently enhance photosynthesis, hence, higher biomass accumulation, especially where there is soil moisture availability. The range of yield reduction for both measured and simulated data with a decline in model accuracy under limited soil moisture conditions (Table 6) has been previously reported [20,24,31,53]. The implication is that the AquaCrop model can adequately predict grain yield under varying environmental conditions. In comparison, however, the higher final maize biomass and grain yield observed in CSA treatments could also be attributed to higher rainfall, which increased soil moisture storage and enhanced maize growth. The higher rainfall and lower temperatures could have promoted canopy growth and biomass accumulation [54], thus reducing evapotranspiration and higher final biomass and grain yields.

The results of the model performance on simulation of ET_c and WUE under different CSA practices are similar to previous reports, which showed that the AquaCrop model systematically underestimated the seasonal ET, and relative changes with the declining soil moisture content [55–57]. Moreover, the change between estimated and simulated ET_c obtained during the current study are higher than those reported by De et al. [15,58], but less than those reported by Katerji et al. [15] while using the AquaCrop model to simulate maize growth under low soil moisture conditions. This could be attributed to differences and variability in soil properties, soil moisture storage, climatic conditions, and crop varieties.

The results indicated no consensus of the deviations in WUE values being a function of the level of plant water shortages. However, measured WUE was higher in the CSA practices, indicating a potential for water saving, given the observed field measurements in the CSA treatments. Moreover, relatively higher values of maize grain yield and biomass were obtained in the CSA practices than in the control treatment (Table 7). The simulated values of WUE achieved during the study are similar to those of previous studies using maize in varying environmental conditions [41]. The relative changes also observed with the AquaCrop model simulated WUE from measured values and R^2 is relatively lower than those previously reported [40,58]. This implies that there is considerable room for improvement in the model estimation of WUE, which relies heavily on predictions of crop ET under well-watered conditions [50], but performs poorly in cases of low soil moisture shortages and severe moisture stress [24].

The calibration process showed higher efficiency of the AquaCrop model in simulation of the *ETc* and WUE (Table 8), probably due to the effectiveness of CSA practices arising from residual effect. This suggests that once the model is calibrated properly, the AquaCrop can reliably predict these variables in environments extremely variable in weather conditions, and the calibrated model can work reasonably well across seasons. The relative error percentage between the simulated and measured values for both *ETc* and WUE was generally in the ranges previously reported in studies [4,58,59]. This implies that the model reliability for these water variables decreases when challenged by extreme weather variations such as intense rainfall events, and, therefore, model improvement is required for better performance.

In the current era of climate change, climate smart agriculture (CSA) practices enhance resilience and combat water shortages through mitigating risks of soil evaporation, e.g., mulch and permanent planting basins. This is an alternative towards soil water conservation in a changing climate. Feeding the growing population requires increase in agriculture productivity as a pre-requisite to food security, which is possible through adoption of CSA practices to reduce negative impacts of climate change in agriculture, hence, alleviating hunger and poverty, a key contribution to realization of sustainable development goals (SDGs), especially zero hunger, climate action, and poverty eradication among smallholder farmers and successful implementation of the 2015 Paris agreement on climate change mitigation and adaptation.

5. Conclusion

The AquaCrop was robust to predict maize yield with the selected climate smart agriculture (CSA) practices as indicated by the statistical indicators with a high degree of accuracy. The AquaCrop model adequately predicts final biomass and grain yield under different CSA practices and this can be a reliable tool in prioritizing climate smart agriculture practices and informing the choice of CSA adoption. Such information is important in enhancing maize productivity and sustainable agriculture production. Furthermore, the study has demonstrated that the AquaCrop model could be used to predict maize biomass and yield with a high degree of reliability and, therefore, the validated model can be used for evaluating the effects of sowing dates on grain yield and biomass. Thus, the model is a valuable tool to inform decision makers on the selection of suitable CSA practices for improved maize production in rainfed production systems. The study was conducted in one agroecological zone and for a short period, future studies would be crucial to assess the AquaCrop model in different agroecological zones over mid to long term periods.

Author Contributions: A.Z., J.G.M.M., B.T. and B.B., background and methodology; A.Z. and R.A.d.S., software and modelling; A.Z., validation; A.Z., R.A.d.S. and A.Z., formal analysis; A.Z., investigation; A.Z., data curation; A.Z. and J.G.M.M., writing—original draft preparation; J.G.M.M., B.T., B.B. and D.B., writing—review and editing; J.G.M.M., B.T. and B.B. and D.B. All authors have read and agreed to the published version of the manuscript.

Funding: Africa Centre of Excellence for Climate Smart Agriculture and Biodiversity Conservation, Haramaya University, Ethiopia. The research is part of a PhD study.

Institutional Review Board Statement: Not applicable.

Informed Consent Statement: Not applicable.

Data Availability Statement: Not applicable.

Acknowledgments: The authors acknowledge support from the Eastern and Southern Africa Higher Education Center of Excellence under the frame of Africa Centre of Excellence for Climate Smart Agriculture and Biodiversity Conservation.

Conflicts of Interest: The authors declare no conflict of interest.

References

- van Dijk, M.; Morley, T.; Rau, M.L.; Saghai, Y. A meta-analysis of projected global food demand and population at risk of hunger for the period 2010–2050. *Nat. Food* **2021**, *2*, 494–501. [CrossRef]
- Jayne, T.S.; Chamberlin, J.; Headey, D.D. Land pressures, the evolution of farming systems, and development strategies in Africa: A synthesis. *Food Policy* **2014**, *48*, 1–17. [CrossRef]
- Epule, T.E.; Ford, J.D.; Lwasa, S. Projections of maize yield vulnerability to droughts and adaptation options in Uganda. *Land Use Policy* **2017**, *65*, 154–163. [CrossRef]
- Greaves, G.E.; Wang, Y.M. Assessment of FAO aquacrop model for simulating maize growth and productivity under deficit irrigation in a tropical environment. *Water* **2016**, *8*, 557. [CrossRef]
- Zizinga, A.; Kangalawe, Y.M.; Ainslie, A.; Tenywa, M.M.; Saronga, N.J.; Amoako, E.E. Analysis of Farmer's Choices for Climate Change Adaptation Practices in South-Western Uganda, 1980–2009. *Climate* **2017**, *5*, 89. [CrossRef]
- Mibulo, T.; Kiggundu, N. Evaluation of FAO aquacrop model for simulating rainfed maize growth and yields in Uganda. *Agronomy* **2018**, *8*, 238. [CrossRef]
- Kaizzi, K.C.; Byalebeka, J.; Semalulu, O.; Alou, I.; Zimwanguyizza, W.; Nansamba, A.; Musinguzi, P.; Ebanyat, P.; Hyuha, T.; Wortmann, C.S. Maize Response to Fertilizer and Nitrogen Use Efficiency in Uganda. *Agron. J.* **2012**. [CrossRef]
- FAO. *Climate Smart Agriculture Sourcebook*; FAO: Rome, Italy, 2013. Available online: www.fao.org/docrep/018/i3325e/i3325e.pdf (accessed on 10 September 2021).
- Lipper, L.; Thornton, P.K.; Campbell, B. Climate Smart Agriculture for Food Security. *Nat. Clim. Change*. **2014**, *4*, 1068–1072. [CrossRef]
- Zizinga, A.; Mwanjalolo, J.G.; Tietjen, B.; Bedadi, B.; Gabiri, G.; Luswata, K.C. Effect of Mulching and Permanent Planting Basin Dimensions on Maize (*Zea mays* L.) Production in a Sub-Humid Climate. *Water* **2022**, *14*, 79. [CrossRef]
- Tambo, J.A.; Kirui, O.K. Yield effects of conservation farming practices under fall armyworm stress: The case of Zambia. *Agric. Ecosyst. Environ.* **2021**, *321*, 107618. [CrossRef]
- Zougmore, R.B.; Partey, S.T.; Ouédraogo, M.; Torquebiau, E.; Campbell, B.M. Facing climate variability in sub-Saharan Africa: Analysis of climate-smart agriculture opportunities to manage climate-related risks. *Cah. Agric.* **2018**, *27*, 1–9. [CrossRef]
- Mulinde, C.; Majaliwa, J.G.M.; Twinomuhangi, R.; David, M.; Komutunga, E.; Ampaire, E.; Asiiimwe, J.; Van Asten, P.; Jassogne, L. Perceived climate risks and adaptation drivers in diverse coffee landscapes of Uganda. *NJAS-Wagening. J. Life Sci.* **2018**, *88*, 31–44. [CrossRef]
- Martins, M.A.; Tomasella, J.; Dias, C.G. Maize yield under a changing climate in the Brazilian Northeast: Impacts and adaptation. *Agric. Water Manag.* **2019**, *216*, 339–350. [CrossRef]
- Greaves, G.E.; Wang, Y.M. Identifying irrigation strategies for improved agricultural water productivity in irrigated maize production through crop simulation modelling. *Sustainability* **2017**, *9*, 630. [CrossRef]
- Steduto, P.; Hsiao, T.C.; Fereres, E.; Raes, D. *Crop Yield Response to Water*; Food and Agriculture Organization of the United Nations: Rome, Italy, 2012; ISBN 9789251072745.
- Mkhabela, M.S.; Bullock, P.R. Performance of the FAO AquaCrop model for wheat grain yield and soil moisture simulation in Western Canada. *Agric. Water Manag.* **2012**, *110*, 16–24. [CrossRef]
- Paredes, P.; Wei, Z.; Liu, Y.; Xu, D.; Xin, Y.; Zhang, B.; Pereira, L.S. Performance assessment of the FAO AquaCrop model for soil water, soil evaporation, biomass and yield of soybeans in North China Plain. *Agric. Water Manag.* **2015**, *152*, 57–71. [CrossRef]
- Farahani, H.J.; Izzi, G.; Oweis, T.Y. Parameterization and evaluation of the aquacrop model for full and deficit irrigated cotton. *Agron. J.* **2009**, *101*, 469–476. [CrossRef]
- Foster, T.; Brozović, N.; Butler, A.P.; Neale, C.M.U.; Raes, D.; Steduto, P.; Fereres, E.; Hsiao, T.C. AquaCrop-OS: An open source version of FAO's crop water productivity model. *Agric. Water Manag.* **2017**, *181*, 18–22. [CrossRef]
- Raes, D.; Steduto, P.; Hsiao, T.C.; Fereres, E. AquaCrop—The FAO Crop Model to Simulate Yield Response to Water: II. Main Algorithms and Software Description. *J. Agron.* **2009**, *101*, 438–447. [CrossRef]
- Vanuytrecht, E.; Raes, D.; Steduto, P.; Hsiao, T.C.; Fereres, E.; Heng, L.K.; Garcia, M.; Mejias, P. AquaCrop: FAO's crop water productivity and yield response model *. *Environ. Model. Softw.* **2014**, *62*, 351–360. [CrossRef]
- Kikoyo, D.A.; Nobert, J. Assessment of impact of climate change and adaptation strategies on maize production in Uganda. *Phys. Chem. Earth* **2016**, *93*, 37–45. [CrossRef]
- Katerji, N.; Campi, P.; Mastrorilli, M. Productivity, evapotranspiration, and water use efficiency of corn and tomato crops simulated by AquaCrop under contrasting water stress conditions in the Mediterranean region. *Agric. Water Manag.* **2013**, *130*, 14–26. [CrossRef]
- Toumi, J.; Er-raki, S.; Ezzahar, J.; Khabba, S.; Jarlan, L.; Chehbouni, A. Performance assessment of AquaCrop model for estimating evapotranspiration, soil water content and grain yield of winter wheat in Tensift Al Haouz (Morocco): Application to irrigation management. *Agric. Water Manag.* **2016**, *163*, 219–235. [CrossRef]
- Wortmann, C.S.; Eledu, C.A. An Agroecological Zonation for Uganda: Methodology and Spatial Information. *Network* **1999**, *30*, 34.

27. Mubiru, D.N.; Radeny, M.; Kyazze, F.B.; Zziwa, A.; Kinyangi, J.; Mungai, C. Soils, Environment and Agro-meteorology Unit, National Agricultural Research Laboratories CGIAR Research Program on Climate Change, Agriculture and Food Security Program Department of Extension and Innovation Studies, College of Agricultural and Envir. *Clim. Risk Manag.* **2018**, *22*, 4–21. [[CrossRef](#)]
28. Sawadogo, H. Using soil and water conservation techniques to rehabilitate degraded lands in Northwestern Burkina Faso. *Int. J. Agric. Sustain.* **2011**, *9*, 120–128. [[CrossRef](#)]
29. MAAIF The Republic of Uganda Ministry of Agriculture, Animal Industries and Fisheries: Performance Review Report; 2017; p. 150. Available online: <https://www.agriculture.go.ug/wp-content/uploads/2020/06/MAAIF-Annual-Performance-Report-2017-18.pdf> (accessed on 1 February 2022).
30. Hsiao, T.C.; Steduto, A.P.; Fereres, E. A systematic and quantitative approach to improve water use efficiency in agriculture. *Water Product. Sci. Pract.* **2007**, 209–231. [[CrossRef](#)]
31. Trout, T.J.; DeJonge, K.C. Crop water use and crop coefficients of maize in the great plains. *J. Irrig. Drain. Eng.* **2018**, *144*, 04018009. [[CrossRef](#)]
32. Steduto, P.; Hsiao, T.C.; Raes, D.; Fereres, E. AquaCrop—The FAO Crop Model to Simulate Yield Response to Water: I. Concepts Underlying Principles. *Agron. J.* **2009**, *101*, 426–437. [[CrossRef](#)]
33. Stevens, B.; Diels, J.; Vanuytrecht, E.; Brown, A.; Bayo, S.; Rujweka, A.; Richard, E.; Alois, P.; Swennen, R. Scientia Horticulturae Canopy cover evolution, diurnal patterns and leaf area index relationships in a Mchare and Cavendish banana cultivar under different soil moisture regimes. *Sci. Hortic.* **2020**, *272*, 109328. [[CrossRef](#)]
34. Allen, R.G.; Pereira, L.S.; Raes, D.; Smith, M. *Crop Evapotranspiration—Guidelines for Computing Crop Water Requirements—FAO Irrigation and Drainage Paper 56*; Food and Agriculture Organisation: Rome, Italy, 1998; Volume 300, p. D05109.
35. Kassaye, K.T.; Yilma, W.A.; Fisha, M.H.; Haile, D.H. Yield and Water Use Efficiency of Potato under Alternate Furrows and Deficit Irrigation. *J. Agron.* **2020**, *2020*, 8869098. [[CrossRef](#)]
36. Raes, D.; Geerts, S.; Kipkorir, E.; Wellens, J.; Sahli, A. Simulation of yield decline as a result of water stress with a robust soil water balance model. *Agric. Water Manag.* **2006**, *81*, 335–357. [[CrossRef](#)]
37. Todorovic, M.; Albrizio, R.; Zivotic, L.; Abi Saab, M.T.; Stöckle, C.; Steduto, P. Assessment of aquacrop, cropsyst, and WOFOST models in the simulation of sunflower growth under different water regimes. *Agron. J.* **2009**, *101*, 509–521. [[CrossRef](#)]
38. Delta-T Devices Ltd. User Manual for the Profile Probe Type PR2. 2006, Volume 104. Available online: <https://www.delta-t.co.uk/product/pr2/> (accessed on 10 September 2018).
39. Eijkelkamp Soil and Water Laboratory Permeameter. 2017, 1–15. Available online: <https://en.eijkelkamp.com/products/laboratory-equipment/soil-water-permeameters.html> (accessed on 15 June 2019).
40. Schaap, M.G.; Leij, F.J.; Van Genuchten, M.T. Rosetta: A computer program for estimating soil hydraulic parameters with hierarchical pedotransfer functions. *J. Hydrol.* **2001**, *251*, 163–176. [[CrossRef](#)]
41. Heng, L.K.; Evett, S.R.; Howell, T.A.; Hsiao, T.C. Calibration and testing of FAO aquacrop model for rainfed and irrigated maize. *Agron. J.* **2009**, *101*, 488–498. [[CrossRef](#)]
42. Nash, J.E.; Sutcliffe, J.V. River flow forecasting through conceptual models part I-A discussion of principles. *J. Hydrol.* **1970**, *10*, 282–290. [[CrossRef](#)]
43. Willmott, C.J.; Ackleson, S.G.; Davis, R.E.; Feddema, J.J.; Klink, K.M.; Legates, D.R.; O’donnell, J.; Rowe, C.M. Statistics for the evaluation and comparison of models. *J. Geophys. Res. Ocean.* **1985**, *90*, 8995–9005. [[CrossRef](#)]
44. Loague, K.; Green, R.E. Statistical and graphical methods for evaluating solute transport models: Overview and application. *J. Contam. Hydrol.* **1991**, *7*, 51–73. [[CrossRef](#)]
45. Ranjbar, A.; Rahimikhoob, A.; Ebrahimian, H.; Varavipour, M. Assessment of the AquaCrop Model for Simulating Maize Response to Different Nitrogen Stresses under Semi-arid Climate. *Commun. Soil Sci. Plant Anal.* **2019**, *50*, 2899–2912. [[CrossRef](#)]
46. Gupta, H.V.; Sorooshian, S.; Yapo, P.O. Status of Automatic Calibration for Hydrologic Models: Comparison with Multilevel Expert Calibration. *J. Hydrol. Eng.* **1999**, *4*, 135–143. [[CrossRef](#)]
47. USDA Natural Resources Conservation Service Soils. Available online: https://www.nrcs.usda.gov/wps/portal/nrcs/detail/soils/survey/?cid=nrcs142p2_054167 (accessed on 18 February 2021).
48. Araya, A.; Habtu, S.; Meles, K.; Kebede, A.; Dejene, T. Test of AquaCrop model in simulating biomass and yield of water deficient and irrigated barley (*Hordeum vulgare*). *Agric. Water Manag.* **2010**, *97*, 1838–1846. [[CrossRef](#)]
49. He, Q.; Li, S.; Hu, D.; Wang, Y.; Cong, X. Performance assessment of the AquaCrop model for film-mulched maize with full drip irrigation in Northwest China. *Irrig. Sci.* **2021**, *39*, 277–292. [[CrossRef](#)]
50. Kaumbutho, P.; Mwalley, J.; Nzabi, A.W.; Temesgen, M.; Mawenya, L. Conservation farming strategies in East and Southern Africa: Yields and rain water productivity from on-farm action research. *Soil Tillage Res.* **2009**, *103*, 23–32. [[CrossRef](#)]
51. Campostrini, E.; Schaffer, B.; Ramalho, J.D.; González, J.C.; Rodrigues, W.P.; da Silva, J.R.; Lima, R.S. Environmental factors controlling carbon assimilation, growth, and yield of papaya (*Carica papaya* L.) under water-scarcity scenarios. In *Water Scarcity and Sustainable Agriculture in Semiarid Environment*; Academic Press: Cambridge, MA, USA, 2018; pp. 481–505.
52. Martellozzo, F.; Amato, F.; Murgante, B.; Clarke, K.C. Modelling the impact of urban growth on agriculture and natural land in Italy to 2030. *Appl. Geogr.* **2018**, *91*, 156–167. [[CrossRef](#)]
53. Katerji, N.; Mastrorilli, M. The effect of soil texture on the water use efficiency of irrigated crops: Results of a multi-year experiment carried out in the Mediterranean region. *Eur. J. Agron.* **2009**, *30*, 95–100. [[CrossRef](#)]

54. Zhang, Q.; Wang, Z.; Miao, F.; Wang, G. Dryland maize yield and water-use efficiency responses to mulching and tillage practices. *Agron. J.* **2017**, *109*, 1196–1209. [[CrossRef](#)]
55. Tan, S.; Wang, Q.; Zhang, J.; Chen, Y.; Shan, Y.; Xu, D. Performance of AquaCrop model for cotton growth simulation under film-mulched drip irrigation in southern Xinjiang, China. *Agric. Water Manag.* **2018**, *196*, 99–113. [[CrossRef](#)]
56. Wang, X.; Fan, J.; Xing, Y.; Xu, G.; Wang, H.; Deng, J.; Wang, Y.; Zhang, F.; Li, P.; Li, Z. The effects of mulch and nitrogen fertilizer on the soil environment of crop plants. *Adv. Agron.* **2019**, *153*, 121–173.
57. Araya, A.; Hoogenboom, G.; Luedeling, E.; Hadgu, K.M.; Kisekka, I.; Martorano, L.G. Assessment of maize growth and yield using crop models under present and future climate in southwestern Ethiopia. *Agric. For. Meteorol.* **2015**, *214–215*, 252–265. [[CrossRef](#)]
58. Greaves, G.E.; Wang, Y. Effect of regulated deficit irrigation scheduling on water use of corn in southern Taiwan tropical environment. *Agric. Water Manag.* **2017**, *188*, 115–125. [[CrossRef](#)]
59. Hatfield, J.L. Can Crop Models Identify Critical Gaps in Genetics, Environment, and Management Interactions? *Front. Plant Sci.* **2020**, *11*, 737. [[CrossRef](#)]